Human Breast Cancer Cells Selected for Resistance to Trastuzumab *In vivo* Overexpress Epidermal Growth Factor Receptor and ErbB Ligands and Remain Dependent on the ErbB Receptor Network

Christoph A. Ritter,[1,2] Marianela Perez-Torres,[2] Cammie Rinehart,[2] Marta Guix,[2] Teresa Dugger,[2] Jeffrey A. Engelman,[5,6] and Carlos L. Arteaga[2,3,4]

Abstract

Purpose: We have investigated mechanisms of acquired resistance to the HER2 antibody trastuzumab in BT-474 human breast cancer cells.

Experimental Design: BT-474 xenografts established in athymic nude mice were eliminated by trastuzumab. Continuous cell lines (HR for Herceptin resistant) were generated from tumors that recurred in the presence of continuous antibody therapy.

Results: The isolated cells behaved resistant to trastuzumab in culture as well as when reinjected into nude mice. They retained *HER2* gene amplification and trastuzumab binding and were exquisitely sensitive to peripheral blood mononuclear cells *ex vivo* in the presence of the antibody. The HR cells exhibited higher levels of phosphorylated epidermal growth factor receptor (EGFR) and EGFR/HER2 heterodimers. Phosphorylation of HER2 in HR cells was inhibited by the EGFR tyrosine kinase inhibitors erlotinib and gefitinib. Gefitinib also inhibited the basal association of p85 with phosphorylated HER3 in HR cells. Both inhibitors as well as the dual EGFR/HER2 inhibitor, lapatinib, induced apoptosis of the HR cells in culture. Growth of established HR5 xenografts was inhibited by erlotinib *in vivo*. In addition, the HR cells overexpressed EGFR, transforming growth factor α, heparin-binding EGF, and heregulin RNAs compared with the parental trastuzumab-sensitive cells.

Conclusions: These results are consistent with the inability of trastuzumab to block the heterodimerization of HER2 and suggest that amplification of ligand-induced activation of ErbB receptors is a plausible mechanism of acquired resistance to trastuzumab that should be investigated in primary mammary cancers.

HER2/*neu* (ErbB2) is a member of the ErbB family of transmembrane receptor tyrosine kinases, which also includes the epidermal growth factor (EGF) receptor (EGFR; ErbB1), HER3 (ErbB3), and HER4 (ErbB4). Binding of ligands to the extracellular domain of EGFR, HER3, and HER4 induces the formation of kinase-active homodimers and heterodimers to which activated HER2 is recruited as a preferred partner (1). Although HER2 does not bind any of the ErbB ligands directly, its catalytic activity can potently amplify signaling by ErbB-containing heterodimers via increasing ligand binding affinity and/or receptor recycling and stability (2–5).

Amplification of the *HER2/neu* (*ERBB2*) gene occurs in ~25% of invasive breast cancers and is associated with poor patient outcome (6). Trastuzumab (Herceptin), a humanized monoclonal IgG1 that binds to the ectodomain of HER2, induces clinical responses in HER2-overexpressing breast cancers and prolongs patient survival when combined with chemotherapy (7–13). The clinical efficacy of trastuzumab seems limited to breast cancers that overexpress HER2 as measured by intense membrane staining in the majority of tumor cells with HER2 antibodies (3+ by immunohistochemistry) or excess copies of the *HER2* gene determined by fluorescence *in situ* hybridization. Therefore, HER2 overexpression by immunohistochemistry and/or fluorescence *in situ* hybridization is the biomarker predictive of good odds of response to treatment with the antibody. However, many patients with *HER2* gene-amplified metastatic breast cancers do not respond or eventually escape trastuzumab, suggesting both *de novo* and acquired mechanisms of therapeutic resistance.

Authors' Affiliations: [1]Institute of Pharmacology and Institute of Pharmacy, University of Greifswald, Greifswald, Germany; Departments of [2]Medicine and [3]Cancer Biology and [4]Breast Cancer Research Program, Vanderbilt-Ingram Comprehensive Cancer Center, Vanderbilt University School of Medicine, Nashville, Tennessee; and [5]Massachusetts General Hospital Cancer Center; [6]Department of Systems Biology, Harvard Medical School, Boston, Massachusetts

Received 3/26/07; revised 5/7/07; accepted 6/5/07.

Grant support: NIH R01 grant CA80195 (C.L. Arteaga), National Cancer Institute T32 grant CA78136 (M. Perez-Torres), Breast Cancer Specialized Program of Research Excellence grant P50 CA98131, and Vanderbilt-Ingram Comprehensive Cancer Center support grant P30 CA68485.

The costs of publication of this article were defrayed in part by the payment of page charges. This article must therefore be hereby marked *advertisement* in accordance with 18 U.S.C. Section 1734 solely to indicate this fact.

Note: Supplementary data for this article are available at Clinical Cancer Research Online (http://clincancerres.aacrjournals.org/).

Requests for reprints: Carlos L. Arteaga, Division of Oncology/Vanderbilt University Medical Center, 2220 Pierce Avenue, 777 PRB, Nashville, TN 37232-6307. Phone: 615-936-3524; Fax: 615-936-1790; E-mail: carlos.arteaga@vanderbilt.edu.

doi:10.1158/1078-0432.CCR-07-0701

Several studies have already reported or speculated on potential mechanisms of resistance to trastuzumab. For example, overexpression of the insulin-like growth factor-I receptor or increased levels of insulin-like growth factor-I receptor/HER2 heterodimers (14, 15), which potently activate phosphatidylinositol 3-kinase (PI3K) and its downstream effector Akt, abrogate trastuzumab action when transfected into antibody-sensitive human breast cancer cells. Amplification of the PI3K pathway as a result of loss or low levels of the phosphatase PTEN in primary tumors is also associated with lower odds of response to trastuzumab (16). Exogenous ligands of the EGFR and HER3/4 coreceptors have been shown to rescue from the antiproliferative effect of the antibody (17, 18). This is consistent with structural and cellular data using ErbB receptor ectodomains and different HER2 monoclonal antibodies, which show that trastuzumab is unable to block ligand-induced EGFR/HER2 and HER2/HER3 heterodimers (19, 20). Finally, Anido et al. (21) reported the presence of HER2 COOH-terminal fragments that result from alternative translation initiation from methionines near the transmembrane domain of the full-length receptor molecule. These fragments are kinase active but lack the trastuzumab binding epitope and, therefore, can potentially allow the cancer cell to escape antibody action. Despite these important leads, there is/are no biomarker(s) than can reliably predict lack of benefit from trastuzumab, which in turn can be used for subsequent clinical trial development and/or individual therapeutic decisions.

In this report, we describe the generation of trastuzumab-resistant BT-474 cells *in vivo*. The resistant cells retained *HER2* gene amplification and trastuzumab binding. They exhibited higher levels of phosphorylated EGFR (P-EGFR) and EGFR/HER2 heterodimers as well as overexpression of EGFR, transforming growth factor α (TGFα), heparin-binding EGF, and heregulin RNAs compared with the parental trastuzumab-sensitive cells, suggesting enhanced EGFR-mediated activation of HER2. Small-molecule inhibitors of EGFR and HER2 were effective against the antibody-resistant cells, suggesting that (*a*) they were still dependent on the ErbB receptor network and (*b*) amplification of ligand-induced activation of ErbB receptors is a potential mechanism of acquired resistance to trastuzumab.

Materials and Methods

Cell lines, kinase inhibitors, and antibodies. BT-474 cells were obtained from the American Type Culture Collection and maintained in improved minimal essential medium (IMEM, Life Technologies, Inc.) supplemented with 10% FCS at 37°C in a humidified, 5% CO_2 incubator. Gefitinib was provided by Alan Wakeling (AstraZeneca Pharmaceuticals, Alderley Park, United Kingdom); erlotinib was from Genentech, Inc.; lapatinib was provided by Tona Gilmer (GlaxoSmithKline, Collegeville, PA); and trastuzumab was purchased from the Vanderbilt University Hospital Pharmacy. Human recombinant TGFα was from R&D Systems.

HER2 gene copy/protein levels and antibody binding. *HER2* gene copy number was determined by fluorescence *in situ* hybridization using HER2 Spectrum Orange and CEP17 Spectrum Green probes (Vysis) as described (22). Enumeration of HER2 and CEP17 signals was done on 25 consecutive cells. Images of representative cells were captured at ×630 with a single-bandpass filter for the detection of Spectrum Orange, Spectrum Aqua, or 4′,6-diamidino-2-phenylindole using IP Labs imaging software package (Scanalytics, Inc.). To determine HER2 surface levels, we followed the procedure described by Moulder et al. (18). Cells in Eppendorf tubes (5×10^5 per tube) were washed three times with staining buffer (5% heat-inactivated FCS in PBS) and then treated with either 200 μg/mL Cy3-conjugated trastuzumab or Cy3-conjugated normal mouse IgG (Santa Cruz Biotechnology). Both samples were incubated for 45 min on ice and washed three times with staining buffer. Flow cytometry of Cy3-labeled cells was done using a FACSCalibur flow cytometer (Becton Dickinson).

To determine trastuzumab binding affinity, cells were grown to confluence, then washed twice with cold serum-free medium, and subsequently incubated with 1 ng/mL ^{125}I-trastuzumab (specific activity, 200,000 cpm/μg) with or without increasing concentrations of unlabeled trastuzumab in triplicate wells for 3 h at 4°C while rocking. After three washes on ice with cold PBS, cells were solubilized with 0.5 N NaOH and cell-associated cpm was measured in a Beckman gamma counter. For standardization purposes, we obtained cell counts from unlabeled wells that were handled similarly to wells containing cells labeled with ^{125}I-trastuzumab. Percentage binding = [cpm sample / cpm control (no unlabeled antibody)] × 100; a best curve fit was generated with GraphPad Prism 4 software and the EC_{50} was calculated using a one site competition equation: Y = bottom + (top - bottom) / $1 + 10^{(X - \log EC50)}$, where X is log (concentration) and Y is binding.

Anchorage-independent and three-dimensional growth assays and terminal deoxynucleotidyl transferase–mediated dUTP nick end labeling. Colony-forming assays in 0.8% agarose were done as described previously (23) in the presence or absence of inhibitors. Cells (3×10^4 per dish) in 35-mm dishes were incubated in 5% CO_2 at 37°C for 7 to 10 days. Tumor cell colonies measuring ≥50 μm were counted using the Omnicon tumor colony analyzer (BioLogics, Inc.). For three-dimensional growth assays, cells were seeded in six-well plates (2×10^6 per well) in growth factor-reduced Matrigel (BD Biosciences) diluted 1:3 with IMEM. Inhibitors were added to the medium at the time of cell seeding and replaced every 3 days. Colonies were photographed using an Olympus DP10 camera mounted in an inverted microscope. After 10 to 14 days, cells were trypsinized and counted in a Zeiss Coulter Counter (Beckman Coulter). To measure apoptosis, adherent cells were treated with inhibitors in serum-free medium; after 48 h, both floating and adherent cells were pooled and subjected to terminal deoxynucleotidyl transferase–mediated dUTP nick end labeling analysis using the APO-bromodeoxyuridine kit (Phoenix Flow Systems) as described (REF) following the manufacturer's protocol.

Establishment of resistant xenografts/cells and mouse studies. Five-week-old female BALB/c athymic nude mice (Harlan Sprague-Dawley) were implanted with 0.72 mg, 60-day release, 17β-estradiol pellets (Innovative Research). The next day, ~2×10^7 BT-474 cells suspended in (300 μL) growth factor-reduced Matrigel were injected s.c. in the right flank via a 22-gauge, 1.5-inch needle. Once tumors reached a volume ≥200 mm^3, mice were treated with 20 mg/kg trastuzumab diluted in sterile PBS by i.p. injection twice a week. Tumor diameters were serially measured with calipers and tumor volumes were calculated by the formula: volume = $width^2 \times length / 2$. Tumors that responded completely and then recurred in the presence of maintained therapy with trastuzumab were harvested, minced, and digested with 0.25% trypsin in IMEM containing antibiotics and DNase for 30 min at room temperature. Cell suspensions were filtered through several layers of sterile gauze, washed twice with serum-containing IMEM, and seeded onto tissue culture flasks in IMEM/10% FCS. For therapeutic studies, antibody-sensitive and antibody-resistant cell lines were injected following the same protocol. Once tumors reached a volume ≥250 mm^3, mice were randomly allocated to treatment with PBS, trastuzumab 20 mg/kg i.p. twice a week, or erlotinib 200 mg/kg daily administered via orogastric gavage.

Immunoblot analysis and immunoprecipitation. After washes with ice-cold PBS, cells were scraped into EBC lysis buffer [50 mmol/L Tris-HCl (pH 7.5), 120 mmol/L NaCl, 0.5% NP40, 100 mmol/L NaF, 200 μmol/L Na_3VO_4, 10 μg/mL each aprotinin, leupeptin, phenylmethylsulfonyl fluoride, and pepstatin] and incubated for 20 min at 4°C while rocking.

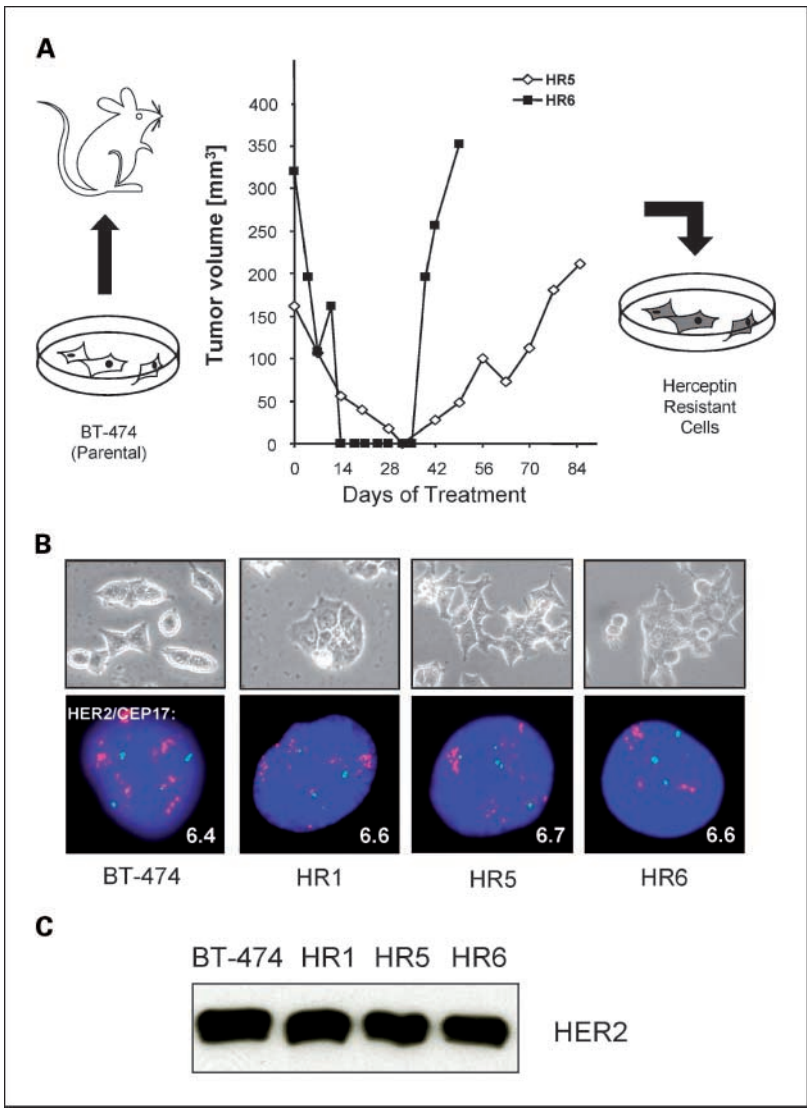

Fig. 1. Selection of trastuzumab-resistant xenografts and cells. *A,* athymic nude mice were injected with $\sim 2 \times 10^7$ BT-474 cells as indicated in Materials and Methods. Mice with established tumors ($\approx$200 mm^3) received trastuzumab 20 mg/kg i.p twice a week. Tumors (four of six) were eliminated and some recurred within the indicated days of treatment (*X axis*) while on continuous therapy with trastuzumab. The recurrent tumors were harvested and minced under sterile conditions. Tumor cell suspensions were prepared and later maintained in IMEM/10% FCS as indicated in Materials and Methods. *B, HER2* gene copy number was determined by fluorescence *in situ* hybridization (*bottom*) as indicated in Materials and Methods. Top, phase microscopy showing epithelial features of cells. Numbers in each panel indicate the ratio of HER2/CEP17 probe signals. *C,* HER2 protein levels as measured by immunoblot analysis of whole-cell lysates from the indicated lines using a HER2 polyclonal antibody. Each lane contains 30 μg of total protein.

Lysates were cleared by centrifugation (10 min at 12,000 rpm, 4°C) and protein concentrations were determined using the bicinchoninic acid assay reagent (Pierce). SDS-PAGE, transfer to nitrocellulose, and immunoblot analysis were done as described previously (24). Horseradish peroxidase–linked IgG (Amersham Pharmacia) was used as secondary antibody. Primary antibodies also used for immunoprecipitation included the following: HER2/*neu* and total EGFR Ab-12 (Neomarkers); phosphorylated tyrosine (P-Tyr) and p85 (Upstate Biotechnology); Y1068 P-EGFR, Y1248 phosphorylated HER2, Y1289 phosphorylated HER3, mitogen-activated protein kinase (MAPK), Akt, and S473 phosphorylated Akt (P-Akt; Cell Signaling); phosphorylated MAPK (P-MAPK; Promega Corp.); and HER3 and HER4 (Santa Cruz Biotechnology). Immunoprecipitations were done as described previously (24) using 0.5 1 mg protein from whole-cell lysates.

Real-time quantitative PCR (Taqman) analysis. RNA was isolated using the Qiagen RNeasy Mini kit. Gene expression was quantified by real-time quantitative PCR or Taqman using 100 ng of total RNA per reaction as described previously (25). The sequences of the primer/probe sets used for this analysis are as follows: EGFR 5′-GCCTTGAGTCATCTATTCAAGCAC-3′ (F), 5′-TGCTACTGTCATTCGCACCTG-3′ (R), and 5′-FAM-AGCTCTGGCCACAACAGGGCATTTT-TAMRA-p-3′ (P); HER2/*neu* 5′-TCTGGACGTGCCAGTGTGAA-3′ (F), 5′-TGCTCCCTGAGGACACATCA-3′ (R), and 5′-FAM-CAGAAGGCCAAGTCCGCAGAAGCC-TAMRA-p-3′ (P); HER3 5′-TTCTCTACTCTACCATTGCCCAAC-3′ (F), 5′-CACCACTATCTCAGCATCTCGGTC-3′ (R), and 5′-FAM-ACACCAACTCCAGCCACGCTCTGCTAMRA-p-3′ (P); HER4 5′-GAGATAACCAGCATTGAGCACAAC-3′ (F), 5′-AGAGGCAGGTAACGAAACTGATTA-3′ (R), and 5′-FAM CCTCTCCTTCCTGCGGTCTGTTCGA-TAMRA-p-3′ (P); EGF 5′-AGCTAACCCATTATGGCAACA-3′ (F), 5′-AGTTTTCACTGAGTCAGCTCCAT-3′ (R), and 5-FAM-AGGGCCCTGGACCCACCAC-TAMRA-p-3′ (P); TGFα 5′-GGACAGCACTGCCAGAGA-3′ (F), 5′-CAGGTGATTACAGGCCAAGTAG-3′ (R), and 5′-FAM-CCTGGGTGTGCCACAGACCTTC-TAMRA-p-3′ (P); HRG 5′-TGGCTGACAGCAGGACTAAC-3′ (F), 5′-CTGGCCTGGATTTCTTC-3′ (R), and 5′-FAM-CAGCAGGCCGCTTCTCGACAC-TAMRA-p-3′ (P); amphiregulin 5′-ATATCACATTGGAGTCACTGCCCA-3′ (F), 5′-GGGTCCATTGTCTTATGATCCAC-3′ (R), and 5′-FAM-AGCCATAAATGATGAGTCGGTCCTCTTTCC-TAMRA-p-3′ (P); heparin-binding EGF, 5′-GAAAGACTTCCATCTAGTCACAAAGA-3′ (F), 5′-GGGAGGCCCAATCCTAGA-3′ (R), and 5-FAM-TCCTTCGTCCCCAGTTGCCG-TAMRA-p-3′ (P); betacellulin 5′-TGCCCCAAGCAATACAAGC-3′ (F), 5′-CGTCTGCTCGGCCACC-3′ (R), 5′-FAM-AAGCGGCATCTCCCTTTGATGCAGTAA-TAMRA-p-3′ (P); and epiregulin 5′-TGCATGCAATTTAAAGTAACTTATTTGACTA-3′ (F), 5′-ATCTTAAGGTACACAATTATCAAAGCTGA-3′ (R), and 5′-FAM-TCGGATTACTGAATTGTATCAATTTGTTTGTGTTCA-TAMRA-p-3′ (P), where F and R are the forward and reverse primers, respectively, and P is the Taqman probe (FAM as reporter and TAMRA as

quencher). Human cDNA FLJ22101 fis (Genbank accession no. AK025754) was used as a housekeeping gene for normalization of EGFR family receptor and ligand gene expression. Primer/probe sets for FLJ22101 are as follows: 5′-TTCCCTGTGGCACTTGACATT-3′ (F), 5′-CTTTTGCCTCTGGCAGTACTCA-3′ (R), and 5′-FAM-TGTCTTAAAGTTTTTGAAGTACATCTTCTGGCCCC-TAMRA-p-3′ (P). Taqman One-Step Universal Master Mix (Applied Biosystems) was used for all reactions. Taqman reaction was done in a standard 96-well plate format with ABI 7500 real-time quantitative PCR system. For data analysis, raw dC_t was first normalized to a housekeeping gene for each sample to get dC_t. The normalized dC_t was then calibrated to BT-474 control to get ddC_t. In the final step of data analysis, the ddC_t was converted to fold change ($2^{-\Delta\Delta Ct}$) relative to control.

Northern hybridization. Total RNA from BT-474, HR5, and HR6 cells was prepared using the RNeasy Mini kit. Twenty micrograms of total RNA per lane were loaded and separated by electrophoresis on 1.2% formaldehyde-agarose gel and transferred to nylon membranes (Hybond N+, Amersham) in 20 × SSC (150 mmol/L NaCl, 15 mmol/L sodium citrate). Prehybridization (2 h) and hybridization (overnight) were carried out in a roller bottle at 50°C in ExpressHyb hybridization solution (BD Biosciences). The hybridized membrane was washed in 2× SSC, 0.1% SDS twice at room temperature, and 0.1× SSC, 0.1% SDS twice at 60°C. Hybridization signals were detected by autoradiography.

TGFα immunoassay. Subconfluent, exponentially growing cells (10^6 cells/60 mm-dish) were incubated in 1 mL of serum-free medium supplemented with 20 μg/mL of the EGFR monoclonal antibody cetuximab (provided by Dan Hicklin, Imclone Systems, Inc., New York, New York) to block EGFR ligand internalization. After 24 h, the medium conditioned by cells was collected and centrifuged at 12,000 rpm for 10 min at 4°C to remove cell debris. TGFα protein in cell conditioned medium was quantitated by sandwich enzyme immunoassay using the TGFα Quantikine kit (R&D Systems). In brief, standards and cell media are added to a 96-well microplate plate coated with a TGFα antibody and incubated for 2 h at room temperature followed by four washes with 0.05% Tween 20 in PBS. A horseradish peroxidase–linked antibody was next added to the wells for additional 2 h. Following another set of washes, a substrate solution containing tetramethylbenzidine was added to the wells with color developing in proportion to the amount of TGFα bound in the initial step. The colorimetric reaction was stopped by acidification with 2 N sulfuric acid and absorbance was measured at 459 and 570 nm. TGFα activity equivalents were calculated from the standard curve and expressed as pg/mL/10^6 cells/24 h.

Peripheral blood cell–induced cytotoxicity. BT-474, HR (for Herceptin resistant), and MDA-468 (HER2 negative) cells were labeled in 24-well plates with 200 μCi/mL $Na_2^{51}CrO_4$ (Amersham Corp.) for 60 min at 37°C; unbound radioactivity was removed after two washes. Single-donor peripheral blood mononuclear cells (PBMC) were isolated from healthy volunteers by Ficoll-Hypaque discontinuous gradient centrifugation and washed twice. Effector PBMCs and ^{51}Cr-labeled (target) cancer cells were coincubated in ratios of 1:1, 3:1, 10:1, and 30:1 in quadruplicate wells in a humidified CO_2 incubator for 4 h at 37°C. Wells containing target cells alone served as controls for spontaneous release (SR) of ^{51}Cr (cell lysis). Labeled cells were counted by

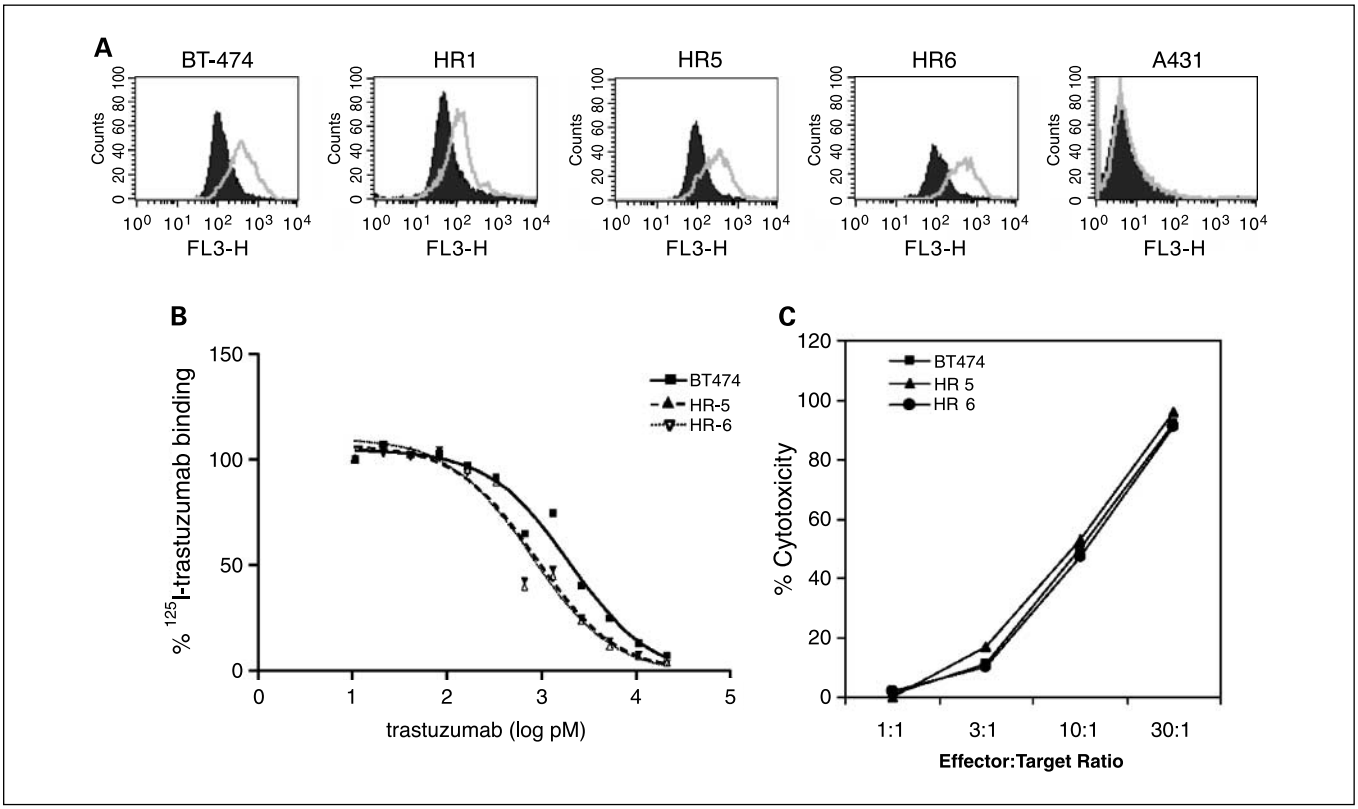

Fig. 2. Trastuzumab-resistant BT-474 cells bind trastuzumab and are sensitive to PBMCs *ex vivo. A,* cell surface levels of HER2 were determined by flow cytometry using Cy3-conjugated trastuzumab. Controls (*shaded areas*) represent cells labeled with Cy3-conjugated normal mouse IgG. Histograms were generated using a FACSCalibur flow cytometer. *B,* confluent monolayers of the indicated cells in 24-well plates were labeled with ^{125}I-trastuzumab for 4 h at 4°C while rocking in the absence or presence of unlabeled trastuzumab (0.001-10 nmol/L). At 4 h, cells were washed with cold PBS three times on ice and harvested with 0.5 N NaOH. Cell-associated cpms were measured in a Beckman gamma counter. Controls indicate cell-associated cpm in the absence of any unlabeled antibody. Points, mean % binding relative to control (no competitor) calculated from three wells. *C,* PBMC-mediated cytotoxicity. BT-474 and HR (target) cells were labeled with ^{51}Cr and then coincubated in different ratios with human PBMCs for 4 h at 37°C. Percentage cytotoxicity as a function of isotope release from target cells was calculated as indicated in Materials and Methods. Points, average of four wells; bars, SD (<5%).

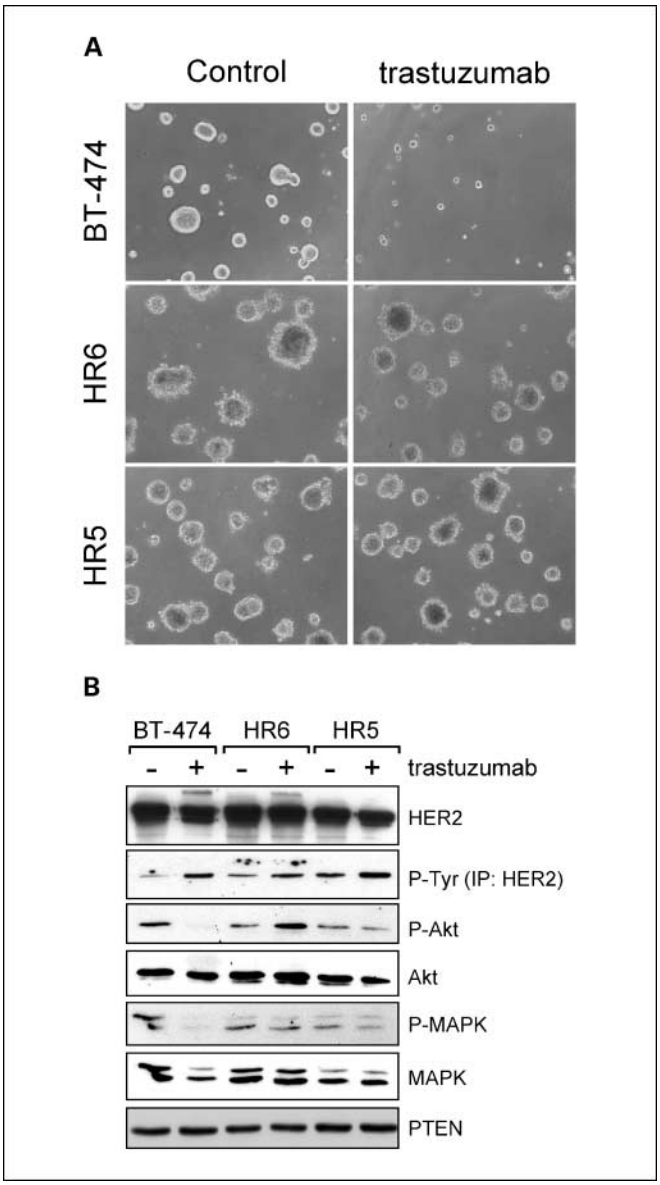

Fig. 3. Trastuzumab does not inhibit postreceptor signals in resistant cells. *A,* cells were seeded in six-well plates in growth factor-reduced Matrigel. The following day, trastuzumab (20 μg/mL) was added and replenished every 72 h. Colonies (≥50 μm) were photographed and counted manually 10 d later. *B,* cells plated as in (*A*) and harvested 24 h after the initial addition of trastuzumab. Whole-cell lysates were prepared, separated by SDS-PAGE, and subjected to immunoblot analysis with the indicated antibodies.

γ scintillography to determine total release (TR) of radioactivity. After centrifugation at 750 × *g* for 10 min at room temperature, the supernatant (SN) was removed for determination of radioactivity. Percentage cytotoxicity was calculated from the formula: 100 × (cpm in SN - SR) / TR - SR.

Results

Trastuzumab-resistant cells retain HER2 overexpression and antibody binding. BT-474 xenografts were established in athymic nude mice and then treated with trastuzumab. Four of six tumors were completely eliminated within 30 days of treatment but some recurred during continuous antibody therapy. Cell lines were established from recurrent (HR) tumors. Two of these (HR5 and HR6) were propagated to study mechanisms of acquired resistance (Fig. 1A). The isolated resistant cells maintained an epithelial morphology similar to that of the parental cells and without any evidence of mouse cell contamination (Fig. 1B, *top*). We examined *HER2* gene amplification by fluorescence *in situ* hybridization using a method that determines oncogene copy number corrected to the number of copies of chromosome 17. BT-474 and all HR sublines exhibited ~6-fold *HER2* gene amplification (Fig. 1B, *bottom*). HER2 protein levels by immunoblot analysis of whole-cell lysates were also similar among sensitive and resistant cells (Fig. 1C).

We next determined if the resistant cells expressed HER2 at the cell surface and were able to bind trastuzumab. Cells were incubated with Cy3-trastuzumab and fluorescence intensity compared with Cy3-labeled nonspecific IgG (control) using flow cytometry. Similar shifts in fluorescence intensity were observed for the trastuzumab-resistant cells compared with BT-474 cells. A single monotypic HR cell population was identified by flow cytometry, indicating an absence of contaminating mouse cells. (Fig. 2A). To estimate binding affinity, cells were labeled with ^{125}I-trastuzumab in the absence or presence of increasing concentrations of unlabeled antibody under conditions that avoid receptor endocytosis. Total binding was similar in BT-474, HR5, and HR6 cells, 10 nmol/L (15 μg/mL) of antibody, eliminating labeled trastuzumab binding completely. Lower concentrations of unlabeled trastuzumab (~1 nmol/L) outcompeted 50% (EC_{50}) of ^{125}I-antibody binding in HR5 and HR6 cells compared with BT-474 cells (~3 nmol/L; Fig. 2B), suggesting that trastuzumab binding affinity was not impaired in the resistant cells.

Antibody-dependent cell-mediated cytotoxicity (ADCC) has been proposed as a dominant component of trastuzumab action. ADCC requires high-affinity binding of the antibody to HER2 in oncogene-overexpressing cells and the recruitment of FcγRIII-expressing immune effector cells, which in turn mediate cell lysis of the tumor target cells (26). Thus, to examine the consequences of antibody binding as they apply to ADCC and a differential sensitivity of the resistant cells to immune cells, we coincubated ^{51}Cr-labeled BT-474 and HR cells with human PBMCs. All three cell lines exhibited identical percentage cytotoxicity when incubated with increasing numbers of effector cells (Fig. 2C), suggesting that the HR cells were not intrinsically resistant to ADCC. No cytotoxicity was observed when using PBMCs and ^{51}Cr-labeled HER2-negative MDA-468 human breast cancer cells in the presence of trastuzumab (data not shown).

HR cells retain resistant phenotype in culture. We determined whether the resistant cells generated in mice retained their phenotype *in vitro*. Cells were plated in Matrigel and followed in the absence or presence of a receptor-saturating concentration of trastuzumab (13 nmol/L). Colony formation of BT-474 cells was markedly reduced (>90%), whereas growth of HR cells was unaffected by treatment with trastuzumab (Fig. 3A). In cell lines, xenografts, and primary breast tumors, trastuzumab has been shown to inhibit activity of postreceptor signal transducers (18, 22, 27, 28) and it has been proposed that these biochemical responses are required for the antitumor action of the antibody against HER2-overexpressing cells. In addition, loss or low levels of PTEN have been associated with trastuzumab resistance (16). Therefore, we examined PTEN content and the effect of trastuzumab on basal activation of MAPK and Akt as measured by antibodies specific to P-MAPK

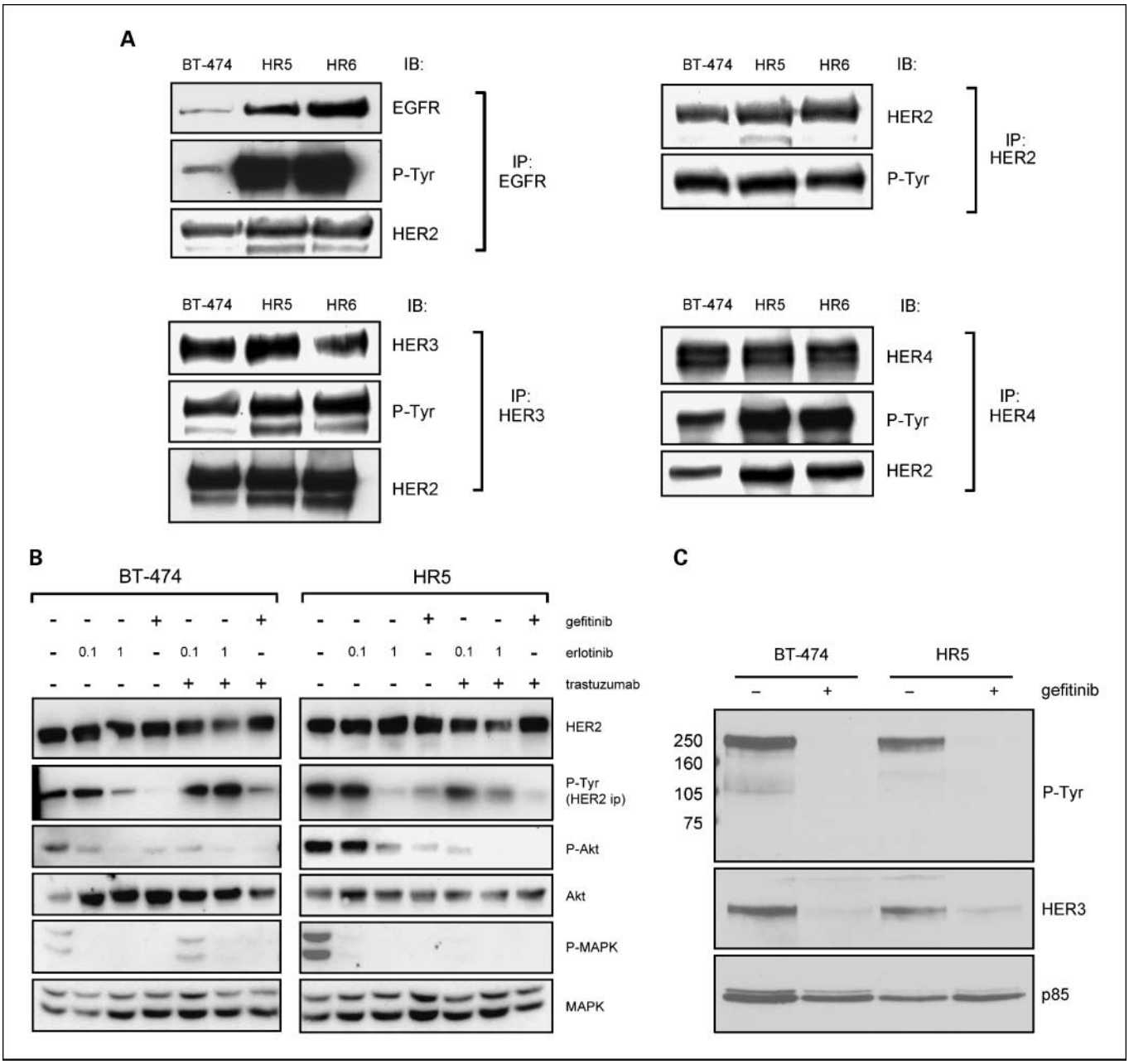

Fig. 4. Trastuzumab-resistant cells express higher levels of EGFR, P-EGFR, and EGFR/HER2 complexes. *A,* subconfluent exponentially growing monolayers were serum-starved overnight and harvested. Cell lysates (500 μg) were precipitated with EGFR, HER2, HER3, or HER4 antibodies. Antibody pulldowns were washed and then subjected to SDS-PAGE followed by immunoblotting with the indicated antibodies. *B,* BT-474 and HR5 cell monolayers were incubated in serum-free medium in the presence or absence of the indicated inhibitors. After 16 h, cells were harvested and whole-cell lysates were subjected to immunoblot analysis with the indicated antibodies. *C,* cells were treated with 1 μmol/L gefitinib for 6 h and then lysed. Cell lysates (500 μg/lane) were precipitated with a p85 antibody as described (59) and immune complexes were subjected to SDS-PAGE followed by immunoblot analysis with P-Tyr, HER3, and p85 antibodies. The ≈200-kDa P-Tyr band comigrated with HER3 and was not recognized by EGFR or HER2 antibodies. Molecular weights in kDa are indicated to the left of the P-Tyr immunoblot.

and S473 P-Akt, respectively. PTEN levels were similar in BT-474 and HR cells. After an overnight incubation and consistent with the effects on three-dimensional growth in Matrigel, trastuzumab treatment inhibited P-MAPK and P-Akt in parental but not in either of the HR sublines (Fig. 3B). Interestingly, a P-Tyr immunoblot of HER2 pulldowns revealed slightly higher phosphorylation of HER2 in the HR cells. In all three cell sublines, this was increased by treatment with the antibody (Fig. 3B).

Trastuzumab-resistant cells overexpress HER2-associated EGFR and remain sensitive to EGFR and HER2 kinase inhibitors. Trastuzumab binds to an epitope in HER2 that is not involved in HER2 heterodimerization with other ErbB receptors (19, 20). Thus, to determine if lateral cross-talk to HER2 was increased in the HR sublines, we examined the levels of phosphorylated EGFR, HER3, and HER4 and their association with HER2 in the resistant cells. ErbB receptors were precipitated with specific antibodies followed by immunoblot

analysis aimed at detecting total and activated receptors as well as their association with HER2. Activated EGFR, HER3, and HER4 were detectable in P-Tyr immunoblots of receptor pulldowns from antibody-sensitive and antibody-resistant cells. EGFR and P-EGFR levels were markedly higher in the HR lines but the levels of HER3 and HER4 remained similar to those in BT-474 cells (Fig. 4A).

To determine if EGFR activation is causally connected to HER2 phosphorylation, we treated cells with the EGFR tyrosine kinase inhibitors (TKI) gefitinib and erlotinib using concentrations that are specific to the receptor kinase and that have been achieved at steady-state levels in the plasma of patients treated with these small molecules (29, 30). Treatment with gefitinib and erlotinib inhibited tyrosine phosphorylation of HER2, P-Akt, and P-MAPK in both BT-474 and HR5 cells (Fig. 4B). In both lines, the combination of trastuzumab with 1 μmol/L erlotinib or gefitinib induced a more complete inhibition than P-Akt compared with the EGFR TKI alone (Fig. 4B, *lanes 6* or *7* or each panel). Similar results were observed in HR6 cells (data not shown). Further, in both cell types, treatment with gefitinib uncoupled p85, the regulatory subunit of PI3K, from a ≈200-kDa P-Tyr band that was recognized by HER3 antibodies (Fig. 4C). These results imply that in the resistant cells, both HER2 and HER3 are transactivated by the EGFR.

We next examined the cytotoxic effect of EGFR inhibition in colony-forming assays and by measuring DNA double-strand breaks in the presence of terminal deoxynucleotidyl transferase and flow cytometry. Treatment with 1 μmol/L gefitinib and erlotinib inhibited anchorage-independent growth of both HR5 and HR6 cells (Fig. 5A). Consistent with these results, evidence of apoptosis was detected in 10% to 15% of cells after a 48-h treatment with the EGFR TKIs but not with trastuzumab (Fig. 5B). We next translated these results to an *in vivo* model by reinjecting HR5 cells into athymic nude mice. All mice formed tumors measuring ≥500 mm^3 within 3 to 4 weeks. Treatment of established HR5 xenografts with trastuzumab did not affect growth whatsoever, whereas administration of erlotinib for 36 days prevented tumor growth. These data suggest that the antibody-resistant tumors are still dependent on the ErbB signaling network and, second, that the resistance to trastuzumab is a stable phenotype in the HR5 cells.

Finally, we tested the effect of lapatinib against HR5 and HR6 cells. This is a reversible dual kinase inhibitor of the EGFR and

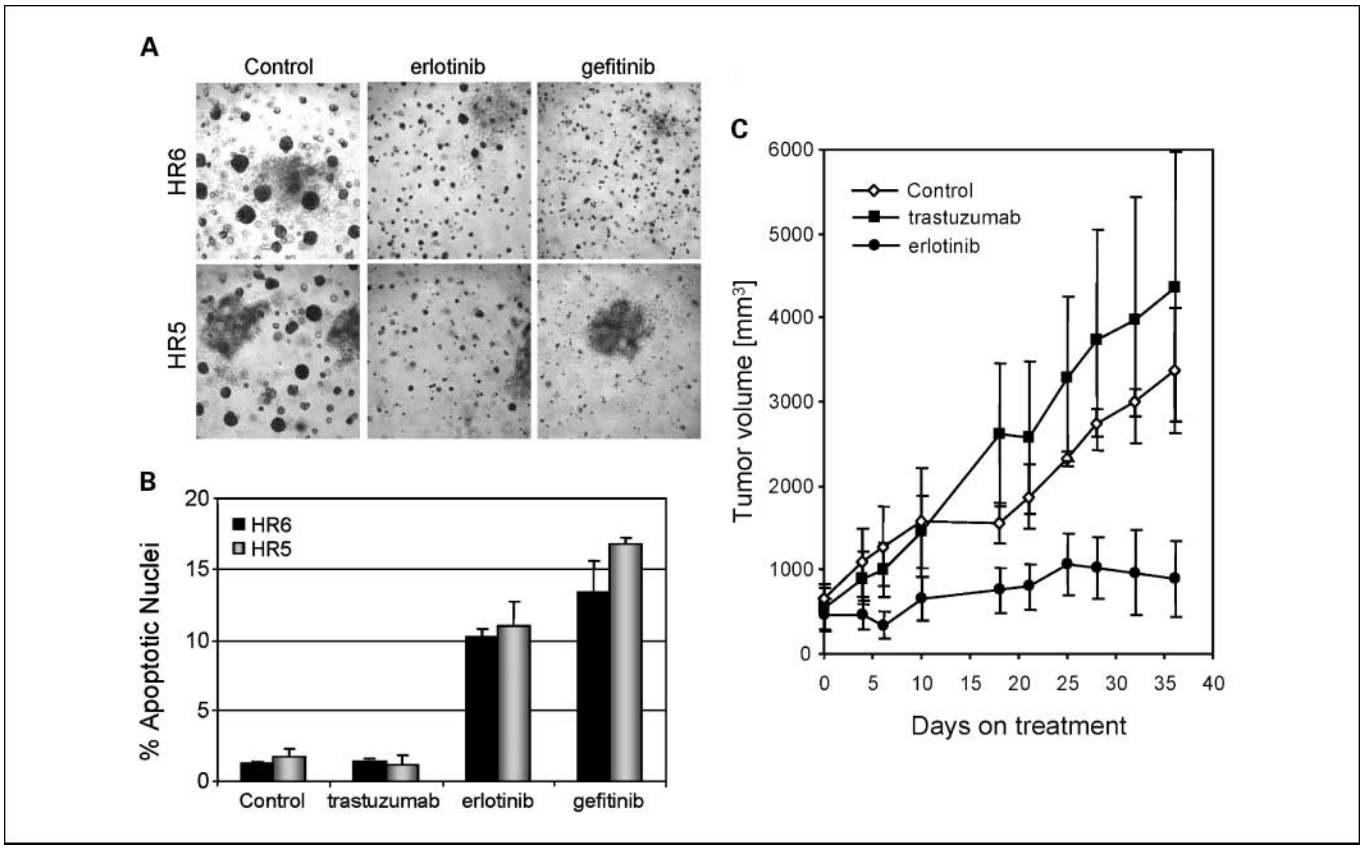

Fig. 5. Trastuzumab-resistant cells are sensitive to EGFR TKIs *in vitro* and *in vivo*. *A,* cells were plated in soft agarose in triplicate 35-mm dishes as indicated in Materials and Methods in the absence or presence of 1 μmol/L erlotinib or gefitinib. Ten days later, colonies were counted manually and photographed. Treatment with the EGFR inhibitors resulted in complete inhibition of colony growth. *B,* cells were seeded in six-well plates in IMEM/10% FCS. The following day, they were changed to serum-free medium ± 1 μmol/L erlotinib or gefitinib or 20 μg/mL trastuzumab. Forty-eight hours later, adherent and floating cells were collected and subjected to TUNEL assay using the APO-bromodeoxyuridine kit. FITC-positive cells were detected by flow cytometry as indicated in Materials and Methods. Columns, mean of three wells; bars, SD. *C,* female athymic nude mice that had been supplemented with estradiol pellets s.c. were injected with HR5 cells into the s.c. space as indicated in Materials and Methods. Once tumors reached a volume ≥500 mm^3, eight mice per group were randomized to no therapy, trastuzumab 20 mg/kg i.p. twice a week, or erlotinib 200 mg/kg daily via orogastric gavage. Tumor diameters were measured serially with calipers and tumor volumes were calculated as indicated in Materials and Methods. Points, mean tumor volume of eight mice per group; bars, SD.

HER2 with potent activity against HER2-overexpressing cancer cells (31, 32). Treatment with lapatinib markedly inhibited three-dimensional growth in Matrigel of BT-474 and the HR sublines (Fig. 6A). Consistent with its cellular activity, lapatinib also inhibited basal Y1248 phosphorylated HER2 and Y1289 phosphorylated HER3 in all three cell lines. Y1068 P-EGFR was detected in HR5 and HR6 but not in BT-474 cells and this site-specific phosphorylation was also eliminated by the addition of lapatinib (Fig. 6B).

Trastuzumab-resistant BT-474 cells overexpress ErbB ligands. To investigate further a possible mechanism to explain the increased activation of EGFRs and EGFR/HER2 complexes, we measured ErbB ligands and receptors by real-time quantitative PCR. Similar to the protein data shown in Fig. 4A, EGFR RNA was markedly up-regulated in both HR sublines compared with parental cells. RNA levels of EGF, TGFα, heparin-binding EGF, and heregulin were also up-regulated in both HR cells. The levels of HER3, betacellulin, and epiregulin were unchanged, whereas amphiregulin RNA was lower in the resistant sublines (Fig. 7A). Northern hybridization also confirmed the up-regulation of TGFα mRNA in HR5 and HR6 cells (Fig. 7B). Secreted TGFα as measured by immunoassay of cell conditioned medium revealed a close to 2-fold increased level of TGFα protein (Fig. 7C). These results suggest that exogenous TGFα would counteract the antitumor effect of the HER2 antibody against BT-474 cells. Therefore, we plated BT-474 cells in soft agarose and added trastuzumab ± TGFα. As predicted, the addition of TGFα to trastuzumab-treated BT-474 cells completed prevented the growth-inhibitory effect of the antibody (Fig. 7D). Similar results were obtained with heregulin (10 ng/mL)–treated BT-474 cells (data not shown).

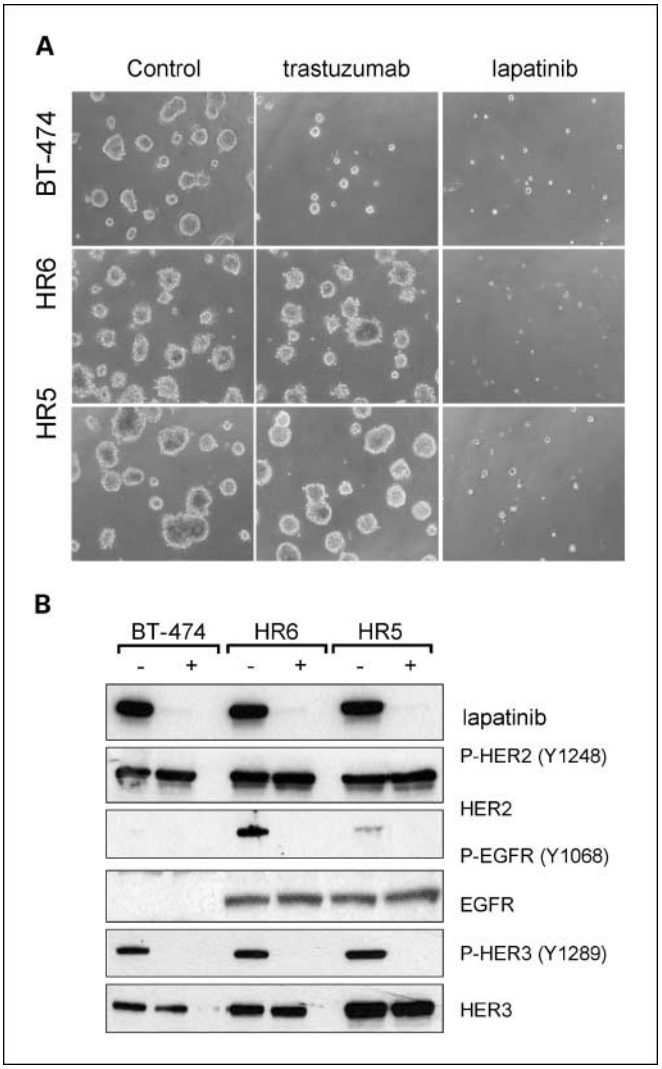

Fig. 6. Trastuzumab-resistant cells remain HER2 dependent. *A,* BT-474. HR6, and HR5 cells were seeded in six-well dishes in Matrigel as in Fig. 3A. The following day, trastuzumab (20 μg/mL) or lapatinib (0.5 μmol/L) was added and replenished every 72 h. Colonies were photographed and counted manually 10 d later. *B,* subconfluent exponentially growing cells were switched from IMEM/10% FCS to serum-free medium and treated or not with 1 μmol/L lapatinib. After an overnight incubation, cells were harvested and lysates were prepared as indicated in Materials and Methods followed by SDS-PAGE and immunoblot analyses with the indicated antibodies. P-HER2, phosphorylated HER2; P-HER3, phosphorylated HER3.

Discussion

Mechanisms involving tumor cells directly as well as host cells have been proposed to explain the inhibitory action of trastuzumab against cancers with high expression of the HER2 oncogene. The antitumor effect of the antibody is almost completely abrogated in mice lacking the receptor FcγRIII (26), strongly implying that ADCC is the main mechanism of action of the IgG1 *in vivo*. The hybridoma (mouse) counterpart of trastuzumab, 4D5, partially removes HER2 from the plasma membrane, potentially preventing its interaction with ErbB coreceptors (33). Two recent articles, however, indicate that trastuzumab does not down-regulate and/or increase the endocytosis of HER2 but, instead, the antibody recycles to the cell surface with the internalized receptor (28, 34). Concurring with these two studies, we did not observe any change in surface HER2 in the resistant cells reported herein by examining levels of HER2 in streptavidin pulldowns from cell surface–biotinylated HR cells (Supplementary Fig. S1).

Other studies have reported an inhibitory effect of trastuzumab on postreceptor signal transduction. Nagata et al. (16) reported antibody-induced recruitment of PTEN to the cell membrane concordant with inhibition of its phosphatase activity by repressing Src-mediated inhibition of PTEN. Trastuzumab treatment inhibits phosphorylation of HER3 and disrupts the basal association of HER3 with HER2 and with p85α resulting in inhibition of PI3K and Akt activities (22). The antisignaling effect of trastuzumab against P-MAPK and P-Akt has also been observed in xenografts and breast primary tumors (18, 27). Suggesting that the inhibition of postreceptor signal transduction is required for trastuzumab action, up-regulation of PI3K and Akt by RNA interference of PTEN and/or overexpression of mutant active Akt confer resistance to trastuzumab (16, 22). Finally, trastuzumab binding blocks the metalloproteinase-mediated cleavage at the juxtamembrane region of HER2 (35), which is associated with the generation of a catalytically active 95-kDa NH_2 terminal fragment of HER2 and shedding of the ectodomain of receptor (36). It remains to be determined whether loss of any of these cellular mechanisms is causally associated with resistance to trastuzumab in patients with breast cancer.

Because of the reported effects of trastuzumab on tumor host cells, specifically the recruitment of immune effector cells via its

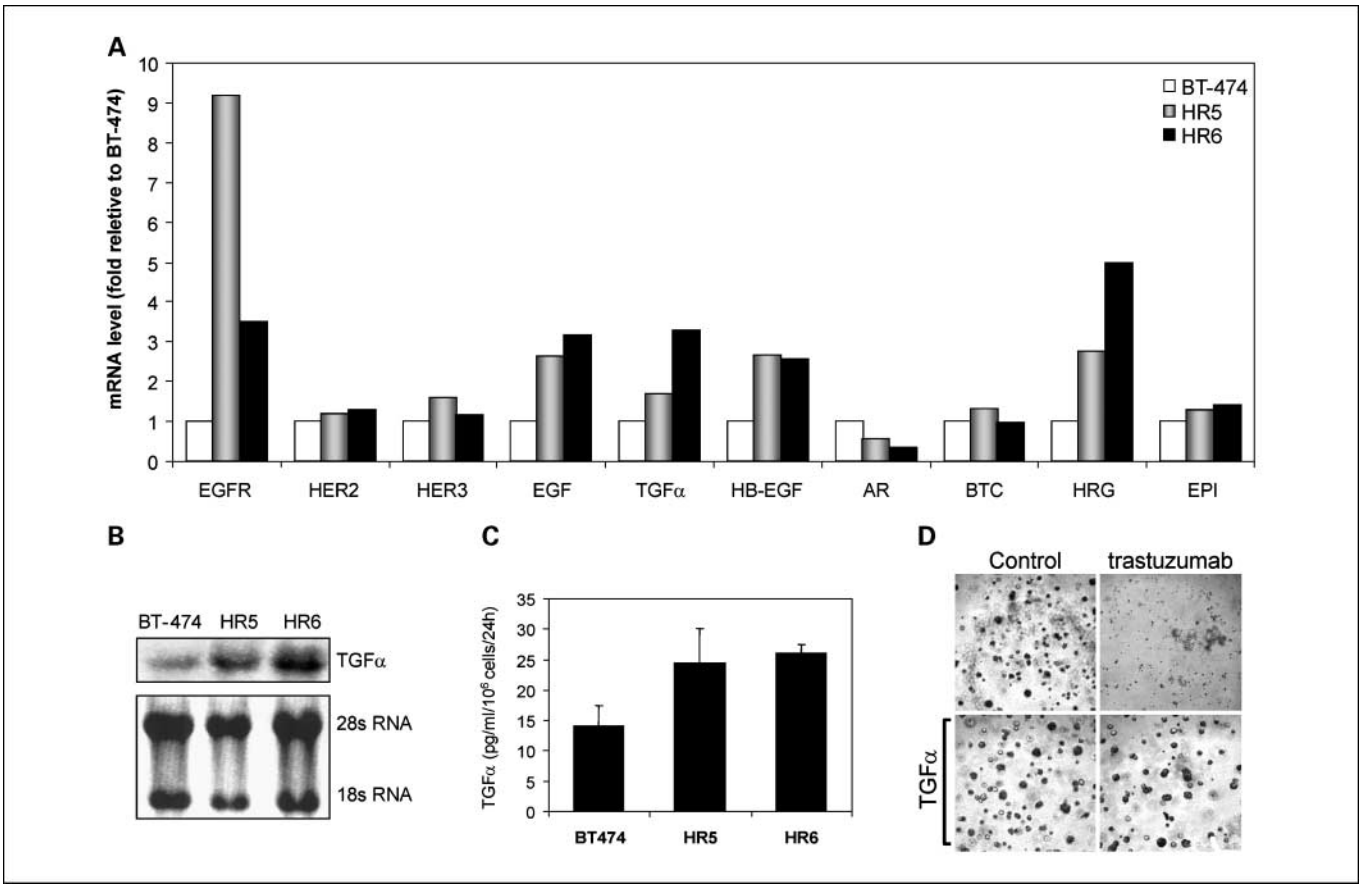

Fig. 7. Trastuzumab-resistant cells overexpress EGFR and ErbB ligands. *A,* total RNA was subjected to quantitative PCR as described in Materials and Methods. Data were normalized to BT-474 control cells. *B,* equal amounts of total RNA harvested from the indicated cells were subjected to Northern hybridization using a ^{32}P-labeled probe for TGFα. The 28S and 18S rRNA bands were used as loading control for the Northern blot. *C,* secretion of TGFα protein was quantitated in cell conditioned medium using an enzyme immunoassay as indicated in Materials and Methods. Data are normalized to pg/mL/10^6 cells/24 h. *D,* exogenous TGFα negates trastuzumab action against antibody-sensitive cells. Parental BT-474 cells were plated in triplicate in a colony-forming assay in the presence of trastuzumab (20 μg/mL) with or without TGFα (10 ng/mL) as indicated in Materials and Methods. Colonies measuring ≥50 μm in diameter were counted 10 d later and photographed using an Olympus DP10 camera.

Fc domain (26) and the inhibition of tumor cell-stimulated endothelial cells (37), we decided to generate antibody-resistant cells in athymic nude mice. Although deficient in T cells, these mice have natural killer cells and macrophages/monocytes, capable of generating ADCC (38). Most established BT-474 xenografts regressed completely on treatment with trastuzumab and some tumors recurred promptly. The (HR) cells isolated from the resistant xenografts retained *HER2* gene amplification and trastuzumab binding and were exquisitely sensitive to PBMCs *ex vivo* in the presence of the antibody, suggesting that they were not intrinsically resistant to ADCC. Their resistant phenotype was retained in culture as well as when reinjected in nude mice. However, they overexpressed EGFR, TGFα, heparin-binding EGF, and heregulin RNAs compared with the parental trastuzumab-sensitive cells. We speculate that the increased EGFR RNA levels are the result of ligand-mediated induction; this autoinduction has been shown in other epithelial cells (39, 40).

In support of EGFR-mediated transactivation of HER2, the HR cells exhibited higher levels of P-EGFR and EGFR/HER2 heterodimers. Second, phosphorylation of HER2 was inhibited by EGFR-specific concentrations of the EGFR TKIs erlotinib and gefitinib. Third, both inhibitors induced significant apoptosis of the HR cells in culture and growth of established HR5 xenografts was inhibited by erlotinib *in vivo*. These results are consistent with the inability of trastuzumab to block the heterodimerization of HER2 with ErbB coreceptors (41). Moreover, in parental and resistant cells, gefitinib disrupted the constitutive association of p85 with HER3 and inhibited P-Akt, further suggesting that activation of PI3K/Akt in the resistant cells remains dependent on the ErbB signaling network via tyrosine phosphorylation of HER3. Notably, we observed antibody-induced phosphorylation of HER2 in both parental and HR cells simultaneous with reduction in P-MAPK and P-Akt (Figs. 3B and 4B). These ligand-like effects have been reported previously with other HER2 (bivalent) monoclonal antibodies but they do not necessarily result in mitogenesis nor negate their antitumor effect (42–45). The significance of this result will require further investigation.

The role of EGFR/HER2 cross-talk in transformation and tumor progression is supported by multiple examples in mouse models and primary human tumors. For example, coexpression of the EGFR ligand TGFα and Neu in the mammary gland of transgenic mice markedly accelerates tumor onset and progression compared with mice expressing Neu or TGFα transgenes alone. In this model, TGFα × Neu bitransgenic mice exhibited increased tyrosine phosphorylation of both EGFR and Neu (46) and tumor latency was markedly delayed by administration of

the EGFR TKI AG-1478 (47). In an analysis of 807 invasive breast cancers, 306 HER2-positive tumors also expressed EGFR by immunohistochemistry. Ninety-seven percent of cancers with phosphorylated HER2 at Y1248 exhibited detectable EGFR and the combination of Y1248 phosphorylated HER2 together with cooverexpression of HER2 and EGFR was associated with the shortest patient survival (48). HER2 is overexpressed in a cohort of non–small cell lung cancers and increased *HER2* gene copy number has been associated with therapeutic response to EGFR TKIs (49, 50).

There is also evidence that amplification of EGFR/HER2 cross-talk, as acquired by the trastuzumab-resistant HR cells, can prevent the antitumor action of the antibody. For example, exogenous EGF, TGFα, betacellulin, and heregulin have been shown to rescue from or attenuate the antiproliferative effect of HER2 antibodies (17, 18, 51). Transfection of a TGFα vector into SKBR-3 cells impairs trastuzumab-induced down-regulation of HER2 (52). MKN7 gastric cancer cells overexpress activated EGFR and are insensitive to 4D5 (53). In these cells, submicromolar concentrations of gefitinib inhibit P-EGFR and restore sensitivity to trastuzumab.[7] To our knowledge, this is the first report in which amplification of EGFR/HER2 cross-talk is associated with acquired resistance to trastuzumab. We surmise that in these complexes, HER2 is still an amplifier of EGFR signals. Thus, as supported by the experiment with lapatinib shown in Fig. 6, we speculate that direct inhibitors of the HER2 kinase will still be effective in this setting. This is consistent with recent reports in which patients with HER-overexpressing tumors that had progressed on trastuzumab responded to the EGFR/HER2 inhibitors lapatinib and HKI-272 (54–56).

Taken together, the results presented herein with *in vivo* selected BT-474 cells suggest that amplification of ligand-induced activation of ErbB receptors is a plausible mechanism of acquired resistance to trastuzumab. This underscores the need to profile levels of ErbB ligands and receptors and, eventually, ErbB receptor heterodimers in HER2-overexpressing tumors treated with trastuzumab not only before therapy but also particularly when acquired resistance occurs. These data also suggest that the combined inhibition of EGFR and HER2 can be synergistic against HER2-overexpressing breast cancers and/or dampen the emergence of acquired resistance. Along those lines, synergy of trastuzumab with the EGFR/HER2 TKI lapatinib (57) and with pertuzumab (58), a HER2 antibody that blocks heterodimerization of HER2 with other ErbB receptors, has been reported in preclinical models and is currently being investigated clinically.

[7] C.L. Arteaga, unpublished data.

References

1. Yarden Y, Sliwkowski MX. Untangling the ErbB signalling network. Nat Rev Mol Cell Biol 2001;2:127–37.
2. Graus-Porta D, Beerli RR, Daly JM, Hynes NE. ErbB-2, the preferred heterodimerization partner of all ErbB receptors, is a mediator of lateral signaling. EMBO J 1997;16:1647–55.
3. Pinkas-Kramarski R, Soussan L, Waterman H, et al. Diversification of Neu differentiation factor and epidermal growth factor signaling by combinatorial receptor interactions. EMBO J 1996;15:2452–67.
4. Wang LM, Kuo A, Alimandi M, et al. H. ErbB2 expression increases the spectrum and potency of ligand-mediated signal transduction through ErbB4. Proc Natl Acad Sci U S A 1998;95:6809–14.
5. Worthylake R, Opresko LK, Wiley HS. ErbB-2 amplification inhibits down-regulation and induces constitutive activation of both ErbB-2 and epidermal growth factor receptors. J Biol Chem 1999;274:8865–74.
6. Ross JS, Fletcher JA. The HER-2/*neu* oncogene in breast cancer: prognostic factor, predictive factor, and target for therapy. Stem Cells 1998;16:413–28.
7. Slamon DJ, Leyland-Jones B, Shak S, et al. Use of chemotherapy plus a monoclonal antibody against HER2 for metastatic breast cancer that overexpresses HER2. N Engl J Med 2001;344:783–92.
8. Vogel CL, Cobleigh MA, Tripathy D, et al. Efficacy and safety of trastuzumab as a single agent in first-line treatment of HER2-overexpressing metastatic breast cancer. J Clin Oncol 2002;20:719–26.
9. Piccart-Gebhart MJ, Procter M, Leyland-Jones B, et al. Trastuzumab after adjuvant chemotherapy in HER2-positive breast cancer. N Engl J Med 2005;353:1659–72.
10. Romond EH, Perez EA, Bryant J, et al. Trastuzumab plus adjuvant chemotherapy for operable HER2-positive breast cancer. N Engl J Med 2005;353:1673–84.
11. Robert N, Leyland-Jones B, Asmar L, et al. Randomized phase III study of trastuzumab, paclitaxel, and carboplatin compared with trastuzumab and paclitaxel in women with HER-2-overexpressing metastatic breast cancer. J Clin Oncol 2006;24:2786–92.
12. Baselga J, Carbonell X, Castaneda-Soto NJ, et al. Phase II study of efficacy, safety, and pharmacokinetics of trastuzumab monotherapy administered on a 3-weekly schedule. J Clin Oncol 2005;23:2162–71.
13. Joensuu H, Kellokumpu-Lehtinen PL, Bono P, et al. Adjuvant docetaxel or vinorelbine with or without trastuzumab for breast cancer. N Engl J Med 2006;354:809–20.
14. Lu Y, Zi X, Zhao Y, Mascarenhas D, Pollak M. Insulin-like growth factor-I receptor signaling and resistance to trastuzumab (Herceptin). J Natl Cancer Inst 2001;93:1852–7.
15. Nahta R, Yuan LX, Zhang B, Kobayashi R, Esteva FJ. Insulin-like growth factor-I receptor/human epidermal growth factor receptor 2 heterodimerization contributes to trastuzumab resistance of breast cancer cells. Cancer Res 2005;65:11118–28.
16. Nagata Y, Lan KH, Zhou X, et al. PTEN activation contributes to tumor inhibition by trastuzumab, and loss of PTEN predicts trastuzumab resistance in patients. Cancer Cell 2004;6:117–27.
17. Motoyama AB, Hynes NE, Lane HA. The efficacy of ErbB receptor-targeted anticancer therapeutics is influenced by the availability of epidermal growth factor-related peptides. Cancer Res 2002;62:3151–8.
18. Moulder SL, Yakes FM, Muthuswamy SK, Bianco R, Simpson JF, Arteaga CL. Epidermal growth factor receptor (HER1) tyrosine kinase inhibitor ZD1839 (Iressa) inhibits HER2/*neu* (erbB2)-overexpressing breast cancer cells *in vitro* and *in vivo*. Cancer Res 2001;61:8887–95.
19. Cho HS, Mason K, Ramyar KX, et al. Structure of the extracellular region of HER2 alone and in complex with the Herceptin Fab. Nature 2003;421:756–60.
20. Agus DB, Akita RW, Fox WD, et al. Targeting ligand-activated ErbB2 signaling inhibits breast and prostate tumor growth. Cancer Cell 2002;2:127–37.
21. Anido J, Scaltriti M, Bech Serra JJ, et al. Biosynthesis of tumorigenic HER2 C-terminal fragments by alternative initiation of translation. EMBO J 2006;25:3234–44.
22. Yakes FM, Chinratanalab W, Ritter CA, King W, Seelig S, Arteaga CL. Herceptin-induced inhibition of phosphatidylinositol-3 kinase and Akt is required for antibody-mediated effects on p27, cyclin D1, and antitumor action. Cancer Res 2002;62:4132–41.
23. Wang SE, Narasanna A, Perez-Torres M, et al. HER2 kinase domain mutation results in constitutive phosphorylation and activation of HER2 and EGFR and resistance to EGFR tyrosine kinase inhibitors. Cancer Cell 2006;10:25–38.
24. Wang SE, Shin I, Wu FY, Friedman DB, Arteaga CL. HER2/Neu (ErbB2) signaling to Rac1-1 is temporally and spatially modulated by transforming growth factor β. Cancer Res 2006;66:9591–600.
25. Heid CA, Stevens J, Livak KJ, Williams PM. Real time quantitative PCR. Genome Res 1996;6:986–94.
26. Clynes RA, Towers TL, Presta LG, Ravetch JV. Inhibitory Fc receptors modulate *in vivo* cytotoxicity against tumor targets. Nat Med 2000;6:443–6.
27. Mohsin SK, Weiss HL, Gutierrez MC, et al. Neoadjuvant trastuzumab induces apoptosis in primary breast cancers. J Clin Oncol 2005;23:2460–8.
28. Longva KE, Pedersen NM, Haslekas C, Stang E, Madshus IH. Herceptin-induced inhibition of ErbB2 signaling involves reduced phosphorylation of Akt but not endocytic down-regulation of ErbB2. Int J Cancer 2005;116:359–67.
29. Baselga J, Rischin D, Ranson M, et al. Phase I safety, pharmacokinetic, and pharmacodynamic trial of ZD1839, a selective oral epidermal growth factor receptor tyrosine kinase inhibitor, in patients with five selected solid tumor types. J Clin Oncol 2002;20:4292–302.
30. Hidalgo M, Siu LL, Nemunaitis J, et al. Phase I and pharmacologic study of OSI-774, an epidermal growth factor receptor tyrosine kinase inhibitor, in patients with advanced solid malignancies. J Clin Oncol 2001;19:3267–79.
31. Rusnak DW, Affleck K, Cockerill SG, et al. The characterization of novel, dual ErbB-2/EGFR, tyrosine kinase inhibitors: potential therapy for cancer. Cancer Res 2001;61:7196–203.
32. Konecny GE, Pegram MD, Venkatesan N, et al. Activity of the dual kinase inhibitor lapatinib (GW572016) against HER-2-overexpressing and

trastuzumab-treated breast cancer cells. Cancer Res 2006;66:1630–9.

33. Hudziak RM, Lewis GD, Winget M, Fendly BM, Shepard HM, Ullrich A. p185HER2 monoclonal antibody has antiproliferative effects *in vitro* and sensitizes human breast tumor cells to tumor necrosis factor. Mol Cell Biol 1989;9:1165–72.

34. Austin CD, De Maziere AM, Pisacane PI, et al. Endocytosis and sorting of ErbB2 and the site of action of cancer therapeutics trastuzumab and geldanamycin. Mol Biol Cell 2004;15:5268–82.

35. Molina MA, Codony-Servat J, Albanell J, Rojo F, Arribas J, Baselga J. Trastuzumab (Herceptin), a humanized anti-Her2 receptor monoclonal antibody, inhibits basal and activated Her2 ectodomain cleavage in breast cancer cells. Cancer Res 2001;61:4744–9.

36. Christianson TA, Doherty JK, Lin YJ, et al. M. NH_2-terminally truncated HER-2/*neu* protein: relationship with shedding of the extracellular domain and with prognostic factors in breast cancer. Cancer Res 1998;58:5123–9.

37. Izumi Y, Xu L, di Tomaso E, Fukumura D, Jain RK. Tumour biology: Herceptin acts as an anti-angiogenic cocktail. Nature 2002;416:279–80.

38. Arteaga CL, Hurd SD, Winnier AR, Johnson MD, Fendly BM, Forbes JT. Anti-transforming growth factor (TGF)-β antibodies inhibit breast cancer cell tumorigenicity and increase mouse spleen natural killer cell activity. Implications for a possible role of tumor cell/host TGF-β interactions in human breast cancer progression. J Clin Invest 1993;92:2569–76.

39. Earp HS, Austin KS, Blaisdell J, et al. Epidermal growth factor (EGF) stimulates EGF receptor synthesis. J Biol Chem 1986;261:4777–80.

40. Earp HS, Hepler JR, Petch LA, et al. Epidermal growth factor (EGF) and hormones stimulate phosphoinositide hydrolysis and increase EGF receptor protein synthesis and mRNA levels in rat liver epithelial cells. Evidence for protein kinase C-dependent and -independent pathways. J Biol Chem 1988;263:13868–74.

41. Franklin MC, Carey KD, Vajdos FF, Leahy DJ, de Vos AM, Sliwkowski MX. Insights into ErbB signaling from the structure of the ErbB2-pertuzumab complex. Cancer Cell 2004;5:317–28.

42. Shawver LK, Mann E, Elliger SS, Dugger TC, Arteaga CL. Ligand-like effects induced by anti-c-erbB-2 antibodies do not correlate with and are not required for growth inhibition of human carcinoma cells. Cancer Res 1994;54:1367–73.

43. Scott GK, Dodson JM, Montgomery PA, et al. p185HER2 signal transduction in breast cancer cells. J Biol Chem 1991;266:14300–5.

44. Harwerth IM, Wels W, Marte BM, Hynes NE. Monoclonal antibodies against the extracellular domain of the erbB-2 receptor function as partial ligand agonists. J Biol Chem 1992;267:15160–7.

45. Kasprzyk PG, Song SU, Di Fiore PP, King CR. Therapy of an animal model of human gastric cancer using a combination of anti-erbB-2 monoclonal antibodies. Cancer Res 1992;52:2771–6.

46. Muller WJ, Arteaga CL, Muthuswamy SK, et al. Synergistic interaction of the Neu proto-oncogene product and transforming growth factor α in the mammary epithelium of transgenic mice. Mol Cell Biol 1996;16:5726–36.

47. Lenferink AE, Simpson JF, Shawver LK, et al. Blockade of the epidermal growth factor receptor tyrosine kinase suppresses tumorigenesis in MMTV/Neu + MMTV/TGF-α bigenic mice. Proc Natl Acad Sci U S A 2000;97:9609–14.

48. DiGiovanna MP, Stern DF, Edgerton SM, Whalen SG, Moore D 2nd, Thor AD. Relationship of epidermal growth factor receptor expression to ErbB-2 signaling activity and prognosis in breast cancer patients. J Clin Oncol 2005;23:1152–60.

49. Hirsch FR, Varella-Garcia M, Franklin WA, et al. Evaluation of HER-2/*neu* gene amplification and protein expression in non-small cell lung carcinomas. Br J Cancer 2002;86:1449–56.

50. Cappuzzo F, Varella-Garcia M, Shigematsu H, et al. Increased HER2 gene copy number is associated with response to gefitinib therapy in epidermal growth factor receptor-positive non-small-cell lung cancer patients. J Clin Oncol 2005;23:5007–18.

51. Diermeier S, Horvath G, Knuechel-Clarke R, Hofstaedter F, Szollosi J, Brockhoff G. Epidermal growth factor receptor coexpression modulates susceptibility to Herceptin in HER2/*neu* overexpressing breast cancer cells via specific erbB-receptor interaction and activation. Exp Cell Res 2005;304:604–19.

52. Valabrega G, Montemurro F, Sarotto I, et al. TGFα expression impairs trastuzumab-induced HER2 downregulation. Oncogene 2005;24:3002–10.

53. Lane HA, Beuvink I, Motoyama AB, Daly JM, Neve RM, Hynes NE. ErbB2 potentiates breast tumor proliferation through modulation of p27(Kip1)-Cdk2 complex formation: receptor overexpression does not determine growth dependency. Mol Cell Biol 2000;20:3210–23.

54. Spector NL, Blackwell K, Hurley J, et al. EGF103009, a phase II trial of lapatinib monotherapy in patients with relapsed/refractory inflammatory breast cancer (IBC): clinical activity and biological predictors of response. Proc Am Soc Clin Oncol 2006;24:3s.

55. Geyer CE, Forste, J, Lindquist D, et al. Lapatinib plus capecitabine for HER2-positive advanced breast cancer. N Engl J Med 2006;355:2733–43.

56. Wong KK, Fracasso PM, Bukowski RM, et al. HKI-272, an irreversible pan erbB receptor tyrosine kinase inhibitor: preliminary phase I results in patients with solid tumors. Proc Am Soc Clin Oncol 2006;24:125s.

57. Xia W, Gerard CM, Liu L, Baudson NM, Ory TL, Spector NL. Combining lapatinib (GW572016), a small molecule inhibitor of ErbB1 and ErbB2 tyrosine kinases, with therapeutic anti-ErbB2 antibodies enhances apoptosis of ErbB2-overexpressing breast cancer cells. Oncogene 2005;24:6213–21.

58. Nahta R, Hung MC, Esteva FJ. The HER-2-targeting antibodies trastuzumab and pertuzumab synergistically inhibit the survival of breast cancer cells. Cancer Res 2004;64:2343–6.

59. Engelman JA, Janne PA, Mermel C, et al. ErbB-3 mediates phosphoinositide 3-kinase activity in gefitinib-sensitive non-small cell lung cancer cell lines. Proc Natl Acad Sci U S A 2005;102:3788–93.

Clinical Cancer Research

Human Breast Cancer Cells Selected for Resistance to Trastuzumab *In vivo* Overexpress Epidermal Growth Factor Receptor and ErbB Ligands and Remain Dependent on the ErbB Receptor Network

Christoph A. Ritter, Marianela Perez-Torres, Cammie Rinehart, et al.

Clin Cancer Res 2007;13:4909-4919.